PHYSICAL REVIEW B **92**, 100501(R) (2015)

Disorder-induced power-law response of a superconducting vortex on a plane

N. Shapira,[1] Y. Lamhot,[1] O. Shpielberg,[1] Y. Kafri,[1] B. J. Ramshaw,[2,*] D. A. Bonn,[2] Ruixing Liang,[2] W. N. Hardy,[2] and O. M. Auslaender[1,†]

[1]*Department of Physics, Technion–Israel Institute of Technology, Haifa, 32000, Israel*

[2]*Department of Physics and Astronomy, University of British Columbia, Vancouver, British Columbia, Canada V6T 1Z1*

(Received 3 January 2014; revised manuscript received 22 April 2015; published 3 September 2015)

We report drive-response experiments on individual superconducting vortices on a plane, a realization for a (1+1)-dimensional directed polymer in random media. For this we use magnetic force microscopy to image and manipulate individual vortices trapped on a twin boundary in $YBa_2Cu_3O_{7-\delta}$ near optimal doping. We find that when we drag a vortex with the magnetic tip, it moves in a series of jumps. As theory suggests, the jump-size distribution does not depend on the applied force and is consistent with power-law behavior. The measured power is much larger than widely accepted theoretical calculations.

DOI: 10.1103/PhysRevB.92.100501 PACS number(s): 74.25.Wx, 68.37.Rt, 74.72.−h, 83.80.Va

While the dynamics of driven systems in ordered media are well understood, disorder gives rise to much more elaborate behavior. Particularly interesting are phenomena arising from the interplay between disorder and elasticity [1,2], such as the conformations of polyelectrolytes [3] (e.g., polypeptides and DNA [4]), kinetic roughening of driven interfaces (e.g., wetting in paper [5,6], magnetic and ferroelectric domain wall motion [7–10], the growth of bacterial colony edges [5]), nonequilibrium effects that occur in randomly stirred fluids [11], and more. Superconducting vortices, in materials in which they behave as elastic strings, are among the most important examples of such systems [12,13]. Despite a dearth of direct experimental proof, these quantized whirlpools of supercurrent are considered textbook examples of the theory of directed polymers in random media (DPRM) [14–16], a foundation model for systems where disorder and elasticity compete. The model, particularly the case of a polymer on a plane [17], yields many results that are believed to be generic and universal and provides the backdrop for our experiment.

Here, we concentrate on vortices that are trapped on a twin boundary (TB), a common planar defect in many high temperature superconductors [18,19]. Such a trapped vortex is widely thought to be a realization of a (1+1)-dimensional directed polymer in random media, which is considered to be well understood theoretically [14]. By using a magnetic force microscope to drag individual vortices, we find that they move in jumps, that the distribution of the jump lengths is independent of the applied force, and that it is consistent with a power law, as suggested by the theory [20]. However, the value for the exponent that we extract from the experiment is significantly larger than the prediction. This implies that the equilibrium theory may not be well suited to describe our driven vortices. The possibility that driving plays a role suggests that even out of equilibrium the system exhibits a robust, scale-free, response.

For a measurement we cool our sample through its superconducting transition temperature T_c in the presence of an external magnetic field $\vec{H} = H\hat{z}$, which directs the curve along which a vortex crosses the sample. Figure 1(a) depicts a vortex away from a TB [V in Fig. 1(a)] that is free to meander in the $d_\perp = 2$ directions perpendicular to $\vec{H}$. For a vortex trapped on a TB [TBV in Fig. 1(a)] the meandering is limited to a plane, i.e., $d_\perp = 1$. This reduced dimensionality is useful because it simplifies the data analysis and thus allows us to track vortex motion in greater detail than if the motion is less restricted [21].

The path of a vortex across a sample is determined by competition between elasticity and disorder: While meandering allows a vortex to lower the energy of the system by locating its core near defects, the associated stretching is limited by finite line tension κ [12]. As a result, the unavoidable random disorder in a sample can make the optimal path for an isolated vortex elaborate. It is interesting to compare our experimental results with the predictions of equilibrium DPRM for disorder-averaged quantities [20]. For example, the thermal- and disorder-averaged offset distance from the field axis $\hat{z}$ [Δ in Fig. 1(a)] scales as a power law given by a universal number called the wandering exponent $\zeta(d_\perp)$: $\overline{\langle\Delta\rangle} \equiv \delta R \sim L^{\zeta(d_\perp)}$ for $L \gg a_z$ (L is the sample thickness, and a_z is a sample-dependent lower cutoff). Theoretically, $\zeta(d_\perp)$ describes a wide variety of systems [14] but only a handful of measurements [7–10,13,22,23]. While a power law also describes classical random walks ($\delta R \sim L^{\frac{1}{2}}$), disorder both enhances wandering [$\zeta(d_\perp) > \frac{1}{2}$] and stretches the distribution $W(\Delta)$ from Gaussian to $W(\Delta) \sim \Delta^{-\alpha_{\text{theory}}}$ ($\alpha_{\text{theory}} > 0$), significantly increasing the prevalence of trajectories with large excursions [20].

The power-law form of $W(\Delta)$ implies the absence of a characteristic length scale and the existence of a significant number of vortex trajectories with a wide variety of Δ's and with free energies almost as low as that of the optimal vortex path. Since these trajectories constitute the low-energy excitations of the system, they are important for thermodynamics and response functions [20]. While in thermal equilibrium the system has time to find these metastable states, it is not clear what happens out of equilibrium, although one can expect that near equilibrium these trajectories remain important.

In this Rapid Communication we experimentally characterize the trajectories of individual vortices confined to move

*Present address: Pulsed Field Facility, Mail Stop E536, Los Alamos National Laboratory, Los Alamos, NM 87545, USA.

†ophir@physics.technion.ac.il

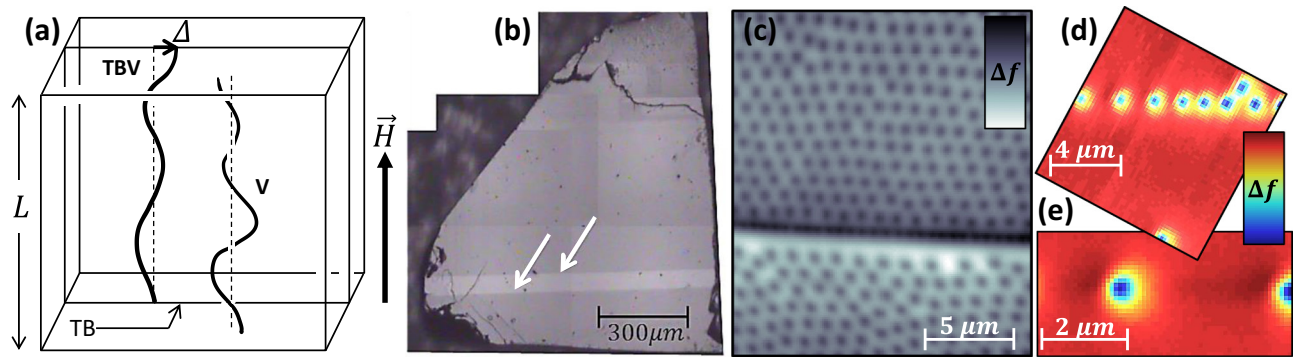

FIG. 1. (Color online) Vortices on and off a twin boundary (TB). (a) Illustration of vortices in a superconductor. The left vortex (V) can meander in $d_\perp = 2$ dimensions perpendicular to an external magnetic field $\vec{H}$ while the vortex trapped on the TB (TBV), a common planar defect, can meander only on the plane, i.e., in $d_\perp = 1$ dimensions. Δ measures how much a vortex meanders from the field axis. (b) Polarized-light microscopy photograph of our 80-μm-thick sample, revealing two TBs (white arrows). (c) MFM scan of vortices (black disks) that form a high density chain along a TB and an Abrikosov lattice around it ($z \approx 1.15$ μm, Δf spans 0.93 Hz). (d) MFM scan at $0 \leqslant H \leqslant 10$ μT. Vortices (blue disks) accumulate on a TB and exhibit $(1+1)$-dimensional physics ($z \approx 0.28$ μm, Δf spans 1.6 Hz). (e) Many vortices in the chain in (d) are isolated because their separation is much larger than $\lambda_{ab} \approx 120$ nm (here, $z \approx 0.4$ μm, Δf spans 0.6 Hz).

on a TB. Unlike most previous work, we use a local probe [magnetic force microscopy (MFM)] to measure individual vortices. The heart of MFM is a sharp magnetic tip situated at the end of a cantilever driven to oscillate along $\hat{z}$ and normal to the sample surface at a resonant frequency f. A force $\vec{F} = F_x\hat{x} + F_y\hat{y} + F_z\hat{z}$ acting on the tip shifts f by $\Delta f = f - f_0 \approx -f_0/(2k)\partial F_z/\partial z$ (f_0 is the natural resonant frequency, k is the cantilever spring constant, and z is the tip-sample distance) [24]. For an image, we record Δf while rastering the tip at constant z. In addition, we use the tip-vortex interaction to perturb vortices individually [25]. Such perturbations show up as abrupt shifts of the signal from a vortex, which we dub "jumps."

The sample we used is a nearly optimally doped $YBa_2Cu_3O_{7-\delta}$ (YBCO) single crystal ($T_c \approx 91$ K [26]) grown from flux in a $BaZrO_3$ crucible for high purity and crystallinity [27]. The $L = 80$ μm thick platelet-shaped sample has faces parallel to the crystal ab plane and contains two parallel TBs [Fig. 1(b)]. Field cooling was done with $\vec{H} = H\hat{z}$ parallel to the crystal c axis and along the TB plane with the tip magnetized for attractive tip-vortex interactions.

Figure 1(c) is an MFM scan of vortex arrays on a TB and around it for $H \approx 2$ mT. Such a highly ordered Abrikosov lattice [28,29] at such a low field attests to the scarcity of strong defects other than the TB. Figure 1(d) is an MFM scan of a TB at $0 \leqslant H \leqslant 10$ μT. In this near-zero field almost all of the vortices were trapped by the TBs, further attesting to the high quality of the sample and in agreement with early experiments showing that, in YBCO, TBs are strong vortex traps [30]. Despite their relative high density, many of the TB vortices can be considered isolated since their nearest-neighbor distance is much larger than the penetration depth $\lambda_{ab} \approx 120$ nm [31] [Fig. 1(e)].

We tested how strongly vortices are trapped by a TB by performing low-height (and hence strong lateral force, up to 20 pN) scans. However, even for our lowest passes across a TB and even for $T \approx 0.85T_c$ we never observed a vortex dislodging from a TB. This experimentally verifies that, for the range of forces we applied, TB vortices behave as one-dimensional (1D) objects in an effective $d = 1 + 1$ geometry.

Next, we performed a series of raster scans over an isolated TB vortex [Fig. 1(e)] in order to perturb it. The scan pattern consisted of line scans in which the tip moved back and forth (Fwd/Bwd) at 125 nm/s along the x axis parallel to the TB. After each line scan we reduced z and stepped the tip in the y direction. Since the force the tip exerts on a vortex depends on both z and the tip-vortex lateral distance $\rho = \sqrt{(x - x_v)^2 + (y - y_v)^2}$ ($x_v\hat{x} + y_v\hat{y}$ is the vortex position in the scan—see Ref. [32]), and since the force binding the vortex to the TB was much stronger than the force we could apply, a complete scan series covering a range of x, y, and z gives the response of a TB vortex to a wide range of forces along the TB, F_x.

Figure 2(a) shows typical line scans for an almost static vortex. Δf becomes increasingly negative as the tip approaches the vortex due to the increasing tip-vortex attraction, until it passes the minimal ρ in the line scan. From there $|\Delta f|$ decreases until the interaction becomes negligible again. The line scans in Fig. 2(a) show one of the first jumps for this particular vortex—a shift in $\Delta f(x)$ at $x = x_{\text{jump}}$. We associate this shift with a tip-induced abrupt change in the position of the upper part of the vortex. We can rule out the possibility that these sharp changes in Δf signal sudden changes in the tip itself because at lower temperatures ($T \approx 4.5$ K), where the tip-vortex interaction is the same but vortices are much less free to move, we never observed sharp changes. We determine the jump length $\Delta_{\text{jump}} = |x_{\text{jump}} - x^*|$ from the first position after the jump satisfying $\Delta f(x^*) = \Delta f(x_{\text{jump}})$ [33]. In addition, we calculate the value of F_x before each jump using an approximation for the magnetic field from a single vortex and a model for the tip [32]. Figure 2(b) shows typical line scans for a moving vortex. While the signal in the central region of the line scan contains numerous sharp changes, the envelope resembles a stretched version of the signal expected from a static vortex at the same z. This indicates that in the central region the top of the vortex moves with the tip in a series of jumps. The observed asymmetry between the Fwd

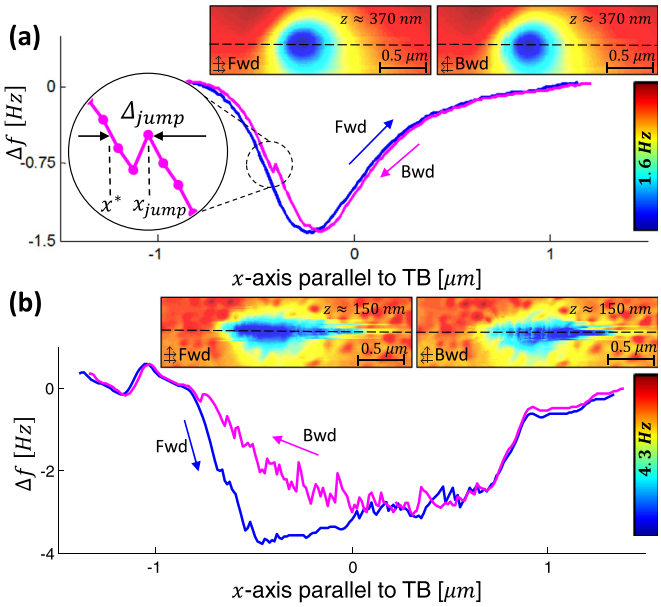

FIG. 2. (Color online) Manipulation scans of TB vortices at $T = 15$ K. (a) Forward (Fwd) and backward (Bwd) line scans (taken along the dashed lines from the scans in the insets) containing a tip-induced vortex jump of size $\Delta_{\text{jump}} = |x^* - x_{\text{jump}}|$ that we associate with an abrupt change in the position of the upper part of the vortex. (b) Fwd and Bwd line scans taken along the dashed lines from the scans in the insets. Numerous vortex jumps with a variety of Δ_{jump}'s are apparent. The difference between the overall shapes of the Fwd and Bwd line scans suggests that nonequilibrium effects may be involved. Insets: The scans from which the line scans in (a) and (b) were taken. The scan height and the span of Δf is indicated for each panel. The horizontal double arrows indicate the back or forth scan direction along the TB (the x axis) and the large vertical arrows indicate the direction we step the tip after each back and forth cycle (the y axis).

and Bwd line scans is typical for a moving vortex and suggests that the system is not in thermal equilibrium.

Figure 3 shows histograms containing all jumps of two vortices chosen for their large separation from their neighbors and each other (enough to safely consider their disorder environments independent). The histograms separate the jumps into three ranges of F_x. When we compare the distribution of Δ_{jump} within each F_x range, we find that the distributions collapse onto each other. Moreover, we find the same collapse when we consider jumps from each vortex separately [34]. This shows that for the range of forces we applied, the distribution of Δ_{jump} does not depend on F_x and justifies lumping all the jumps together, regardless of the force.

Our main result is the force-independent distribution $\tilde{W}(\Delta_{\text{jump}})$ for both vortices together (Fig. 4). The most significant feature of $\tilde{W}(\Delta_{\text{jump}})$ is a long tail, indicating that disorder is important—it is in complete disagreement with the Gaussian distribution expected for a system where disorder is irrelevant [20]. Another important feature is the saturation of α_{fit} obtained from best fits of $\tilde{W}(\Delta_{\text{jump}})$ to a power law for different values of a lower cutoff a_x. The saturation is a strong indication that $\tilde{W}(\Delta_{\text{jump}})$ is a power law for $\Delta_{\text{jump}} > a_0 = 49 \pm 3$ nm with the power given by $\alpha_{\text{meas}} = 2.75 \pm 0.06$ (80% confidence level). We emphasize that we determined

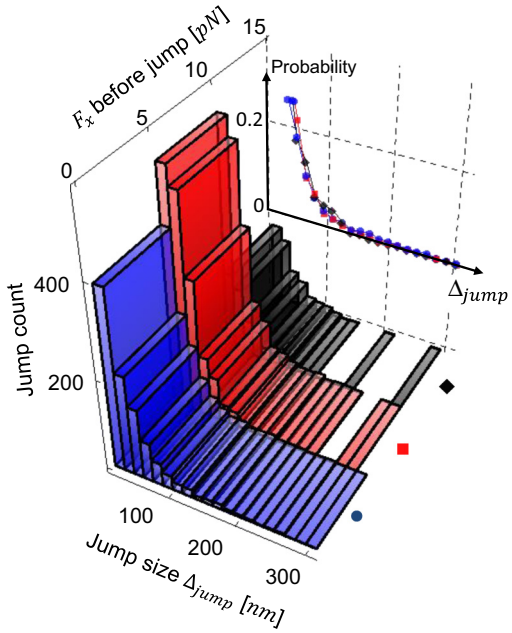

FIG. 3. (Color online) Histograms binning all measured jump lengths (Δ_{jump}) for different ranges of the force exerted along the TB by the tip (F_x). Inset: Normalized distributions of Δ_{jump} for the different F_x ranges. All the distributions collapse onto each other, revealing the independence of Δ_{jump} from F_x.

Δ_{jump} directly and without theoretical assumptions and that $\tilde{W}(\Delta_{\text{jump}})$, α_{meas}, and a_0 are not sensitive to several important sources of systematic error [the independence of $\tilde{W}(\Delta_{\text{jump}})$ on F_x implies that it is not sensitive to systematic errors in force estimates, and the scale invariance of power laws implies that α_{meas} is insensitive to errors in length calibration].

The independence of $\tilde{W}(\Delta_{\text{jump}})$ on F_x (Fig. 3), which at first glance may seem puzzling, is attributed by DPRM theory to

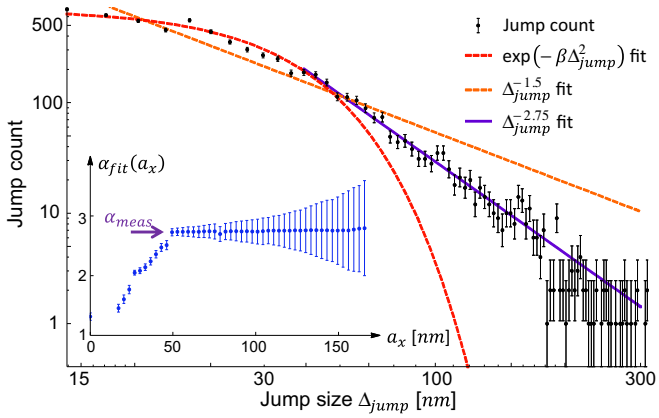

FIG. 4. (Color online) Measured vortex jump lengths (Δ_{jump}) and fits to the data. Although the data are consistent with a power-law distribution, the exponent we obtain does not match $\alpha_{\text{theory}} = 3/2$ predicted for a system in equilibrium. Inset: Values of a power-law exponent α_{fit} obtained by fitting the data in the main panel for different values of the lower cutoff a_x. α_{fit} saturates (arrow) for $a_x > a_0 = 49 \pm 3$, a clear indication that $\alpha_{\text{meas}} = 2.75 \pm 0.06$ is the best-fit exponent for the distribution.

statistical tilt symmetry [20]. This symmetry is a manifestation of the absence of correlations in the disorder, which means that for a sufficiently large force [20], as in this experiment [35], each time we tilt a vortex, it samples a new random environment and is equivalent to an untilted vortex experiencing a new disorder realization. The observed statistical tilt symmetry implies that theoretically we could have obtained disorder-averaged quantities from measurements of just one vortex. Indeed, when we examine the force-independent distributions of Δ_{jump} for each vortex separately [36], we find that the distributions are statistically similar. This observed self-averaging corroborates the statistical tilt symmetry in our system and means that for our system the measured distribution of jump lengths is indeed equivalent to the distribution of rare, large-scale, low-energy excitations, i.e., $\tilde{W}(\Delta_{\text{jump}}) = W(\Delta)$.

While DPRM predicts the power-law behavior of $W(\Delta)$, the value we extract disagrees with the theoretical value: $\alpha_{\text{theory}} = d_\perp + 2 - \zeta^{-1}(d_\perp)$ [20]. The value of the wandering exponent is known exactly for $d_\perp = 1$ to be $\zeta = 2/3$ [37–39], giving $\alpha_{\text{theory}} = 3/2$, very different from $\alpha_{\text{meas}} \approx 2.75$. This deviation could result from a variety of reasons; however, the asymmetry of the line traces in Fig. 2(b) suggests that nonequilibrium effects may be involved. This raises the possibility that the exponent that we measure is enhanced from the expected value because the system does not have time to find the optimal path. The fact that we observe a response that remains power-law distributed even out of equilibrium is surprising. Whether or not nonequilibrium effects in fact explain the enhancement of α_{meas} is a question that requires further study.

The value of the cutoff a_0 provides a way to characterize the statistical properties of the point disorder near a TB. This is due to general scaling arguments that hold both in and out of equilibrium [20] and give a relationship between a_0 and the variance of the disorder potential (D). The precise mechanism for the interaction between vortices and the disorder does not matter as long as it results from defects that are small on the scale of the size of the vortex core [12]. This is the case in pristine YBCO, where the dominant defects off TBs are oxygen vacancies [27,40,41]. In $d = 1 + 1$ one finds $D = (k_B T)^3/(a_0 \kappa)$ (k_B is the Boltzmann constant) [20]. Using $T = 15$ K and $\kappa = 2.4$ eV/μm, we find $\sqrt{D} \approx 135$ μeV [42]. Similar scaling relations give an estimate for the cutoff along z, i.e., $a_z = (a_0^2 \kappa)/(k_B T) \approx 4.5$ μm $\ll L = 80$ μm, consistent with the experiment being in the thick sample regime.

To conclude, we have used the interaction between a magnetic tip and superconducting vortices on a TB to study the behavior of individual directed 1D objects. This provides an ideal setup for studying the interplay between elasticity and disorder, which is ubiquitous in nature. After experimentally showing that vortices on a TB behave as 1D objects in an effective $1 + 1$ random medium, we proceeded to pull them one at a time along the TB and measured the distribution of jump lengths $\tilde{W}(\Delta_{\text{jump}})$. We find that $\tilde{W}(\Delta_{\text{jump}})$ is independent of the force applied by the tip and is the same for two widely separated vortices, confirming the predicted statistical tilt symmetry in the system. Our central result is the power-law form of $\tilde{W}(\Delta_{\text{jump}})$ that suggests that even out-of-equilibrium excitations do not have a characteristic length scale beyond the sample-specific lower cutoff a_0. The direct measurement of a_0 provides a different characterization of the local disorder strength D around the TB, complementing other measures such as the critical current [43,44]. It will be interesting to check if our results can be understood within an alternate theory that accounts for out-of-equilibrium effects.

We thank Thierry Giamarchi, who encouraged us to focus on vortex motion along a TB, as well as Anatoli Polkovnikov, Daniel Podolsky, and Jennifer Hoffman for comments, and Gad Koren for help with characterization. N.S. acknowledges support from the Gutwirth Fellowship and Posnansky Research Fund in High Temperature Superconductivity. Y.L. acknowledges support from the Technion Russell Berrie Nanotechnology Institute (RBNI). O.M.A. acknowledges support by Alon and Horev Fellowships as well as support by the Taub Foundation. The project has received funding from the EU Seventh Framework Programme (FP7/2007-2013) under Grant Agreement No. 268294 and from the Israel Science Foundation under Grant No. 1897/14. Work at UBC is supported by the Natural Sciences and Engineering Research Council as well as the Canadian Institute for Advanced Research.

[1] A. B. Kolton, A. Rosso, T. Giamarchi, and W. Krauth, Phys. Rev. Lett. **97**, 057001 (2006).

[2] E. Agoritsas, V. Lecomte, and T. Giamarchi, Physica B **407**, 1725 (2012).

[3] P.-G. de Gennes, *Scaling Concepts in Polymer Physics* (Cornell University Press, Ithaca, NY, 1979).

[4] C. Bustamante, Z. Bryant, and S. B. Smith, Nature (London) **421**, 423 (2003).

[5] T. Halpin-Healy and Y. Zhang, Phys. Rep. **254**, 215 (1995).

[6] S. Herminghaus, Phys. Rev. Lett. **109**, 236102 (2012).

[7] S. Lemerle, J. Ferré, C. Chappert, V. Mathet, T. Giamarchi, and P. Le Doussal, Phys. Rev. Lett. **80**, 849 (1998).

[8] P. Paruch, T. Giamarchi, and J.-M. Triscone, Phys. Rev. Lett. **94**, 197601 (2005).

[9] M. Yamanouchi, J. Ieda, F. Matsukura, S. Barnes, S. Maekawa, and H. Ohno, Science **317**, 1726 (2007).

[10] K.-J. Kim, J.-C. Lee, S.-M. Ahn, K.-S. Lee, C.-W. Lee, Y. J. Cho, S. Seo, K.-H. Shin, S.-B. Choe, and H.-W. Lee, Nature (London) **458**, 740 (2009).

[11] D. Forster, D. R. Nelson, and M. J. Stephen, Phys. Rev. A **16**, 732 (1977).

[12] G. Blatter, M. V. Feigel'man, V. B. Geshkenbein, A. I. Larkin, and V. M. Vinokur, Rev. Mod. Phys. **66**, 1125 (1994).

[13] C. A. Bolle, V. Aksyuk, F. Pardo, P. L. Gammel, E. Zeldov, E. Bucher, R. Boie, D. J. Bishop, and D. R. Nelson, Nature (London) **399**, 43 (1999).

[14] M. Kardar, *Statistical Physics of Fields* (Cambridge University Press, Cambridge, UK, 2007).

[15] V. S. Dotsenko, L. B. Ioffe, V. B. Geshkenbein, S. E. Korshunov, and G. Blatter, Phys. Rev. Lett. **100**, 050601 (2008).
[16] T. Halpin-Healy, Phys. Rev. Lett. **109**, 170602 (2012).
[17] T. Hwa, Nature (London) **399**, 17 (1999).
[18] H. Hilgenkamp and J. Mannhart, Rev. Mod. Phys. **74**, 485 (2002).
[19] M. A. Tanatar, A. Kreyssig, S. Nandi, N. Ni, S. L. Bud'ko, P. C. Canfield, A. I. Goldman, and R. Prozorov, Phys. Rev. B **79**, 180508 (2009).
[20] T. Hwa and D. S. Fisher, Phys. Rev. B **49**, 3136 (1994).
[21] O. M. Auslaender, Lan Luan, E. W. J. Straver, J. E. Hoffman, N. C. Koshnick, E. Zeldov, D. A. Bonn, Ruixing Liang, W. N. Hardy, and K. A. Moler, Nat. Phys. **5**, 35 (2009).
[22] K. A. Takeuchi and M. Sano, Phys. Rev. Lett. **104**, 230601 (2010).
[23] K. A. Takeuchi, M. Sano, T. Sasamoto, and H. Spohn, Sci. Rep. **1**, 34 (2011).
[24] T. R. Albrecht, P. Grütter, D. Horne, and D. Rugar, J. Appl. Phys. **69**, 668 (1991).
[25] E. W. J. Straver, J. E. Hoffman, O. M. Auslaender, D. Rugar, and K. A. Moler, Appl. Phys. Lett. **93**, 172514 (2008).
[26] See Supplemental Material at http://link.aps.org/supplemental/10.1103/PhysRevB.92.100501 for the transition temperature T_c and Meissner repulsion.
[27] Ruixing Liang, D. A. Bonn, and W. N. Hardy, Physica C **304**, 105 (1998).
[28] A. A. Abrikosov, Zh. Eksp. Teor. Fiz. **32**, 1442 (1957) [JETP **5**, 1174 (1957)].
[29] W. H. Kleiner, L. M. Roth, and S. H. Autler, Phys. Rev. **133**, A1226 (1964).
[30] L. Vinnikov, L. A. Gurevich, G. A. Yemelchenko, and Y. Ossipyan, Solid State Commun. **67**, 421 (1988).
[31] R. F. Kiefl, M. D. Hossain, B. M. Wojek, S. R. Dunsiger, G. D. Morris, T. Prokscha, Z. Salman, J. Baglo, D. A. Bonn, Ruixing Liang, W. N. Hardy, A. Suter, and E. Morenzoni, Phys. Rev. B **81**, 180502 (2010).
[32] See Supplemental Material at http://link.aps.org/supplemental/10.1103/PhysRevB.92.100501 for the force formula.
[33] See Supplemental Material at http://link.aps.org/supplemental/10.1103/PhysRevB.92.100501 for the jump detection algorithm.
[34] See Supplemental Material at http://link.aps.org/supplemental/10.1103/PhysRevB.92.100501 for self-averaging of tilted vortices.
[35] See Supplemental Material at http://link.aps.org/supplemental/10.1103/PhysRevB.92.100501 for minimum tilt for self-averaging.
[36] See Supplemental Material at http://link.aps.org/supplemental/10.1103/PhysRevB.92.100501 for force-independent self-averaging of tilted vortices.
[37] M. Kardar, Nucl. Phys. B **290**, 582 (1987).
[38] D. A. Huse, C. L. Henley, and D. S. Fisher, Phys. Rev. Lett. **55**, 2924 (1985).
[39] L.-H. Gwa and H. Spohn, Phys. Rev. A **46**, 844 (1992).
[40] Ruixing Liang, D. A. Bonn, and W. N. Hardy, Physica C **336**, 57 (2000).
[41] Ruixing Liang, D. A. Bonn, and W. N. Hardy, Phys. Rev. B **73**, 180505(R) (2006).
[42] See Supplemental Material at http://link.aps.org/supplemental/10.1103/PhysRevB.92.100501 for the line tension κ.
[43] S. R. Foltyn, L. Civale, J. L. MacManus-Driscoll, Q. X. Jia, B. Maiorov, H. Wang, and M. Maley, Nat. Mater. **6**, 631 (2007).
[44] S. H. Wee, Y. L. Zuev, C. Cantoni, and A. Goyal, Sci. Rep. **3**, 2310 (2013).